Nebojša Gnjatović
Assistant Professor
University of Belgrade
Faculty of Mechanical Engineering

Srđan Bošnjak
Professor
University of Belgrade
Faculty of Mechanical Engineering

Ivan Milenović
Research Assistant
University of Belgrade
Faculty of Mechanical Engineering

Aleksandar Stefanović
Research Assistant
University of Belgrade
Faculty of Mechanical Engineering

Marko Urošević
Research Assistant
University of Belgrade
Faculty of Mechanical Engineering

Gantry Bucket Chain Stacker-Reclaimer for Crushed Gypsum

Stackers-reclaimers represent the mechanization backbone of high-capacity storages for granular materials. The paper presents the design of a gantry bucket chain stackers-reclaimer for handling of crushed gypsum, as well as the working technology, finite element strength calculation for the main substructures: the working device, the trolley and the gantry. Failureless operation of the presented stacker-reclaimer represent an indirect validation of not only the presented results, but also the entire project as well as the applied technology of manufacture and montage.

Keywords: *stacker-reclaimer, design, working technology, structure, strength.*

1. INTRODUCTION

Stackers-reclaimers (S-R) represent the backbone of mechanization in high-capacity storages for granular materials [1,2]. This class of machines is used in coal supply systems of thermal power plants [3-5], as well as subsystems for storage and transport of gypsum, a byproduct of desulfurization of exaust gases. A bridge-type bucket chain S-R, "USKL" (producted by "IVA Process Equipment" – Aranđelovac, Serbia), Figures 1 and 2, Table 1, was designed for the supplying of the storage of crushed gypsum at the thermal power plant "Kostolac A".

Table 1. Basic technical data

Capacity	240 t/h
Span	8 m
Overhang	5.88 m
Total height	12.6 m
Track length	85 m
Total installed power	88.8 kW

Figure 1. S-R USKL right after the assembly

Correspondence to: Dr John Smith, associate professor
Faculty of Mechanical Engineering,
Kraljice Marije 16, 11120 Belgrade 35, Serbia
E-mail: jsmith@mas.bg.ac.rs

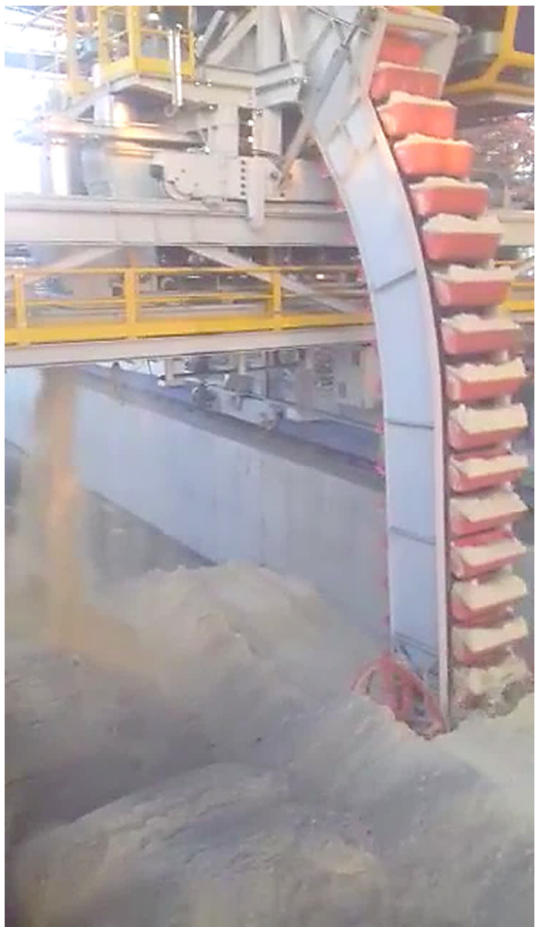

Figure 2. S-R USKL in test operation

2. MAIN SUBASSEMBLIES OF THE S-R USKL

The main functional subsystems of the S-R USKL, Figure 3, are: the load-bearing structure-gantry (1); the movement mechanism for the S-R (2); the trolley (3) with the working device (4); the subsystem for transport of the material: a mobile belt conveyor (5) on the gantry, a hanging belt conveyor (6) on the trolley (3), and the cascade discharge device; a subsystem for

dedusting (7) at the transfer points; the control subsystem (8) inside the operator's cabin (9), and the electro-equipment.

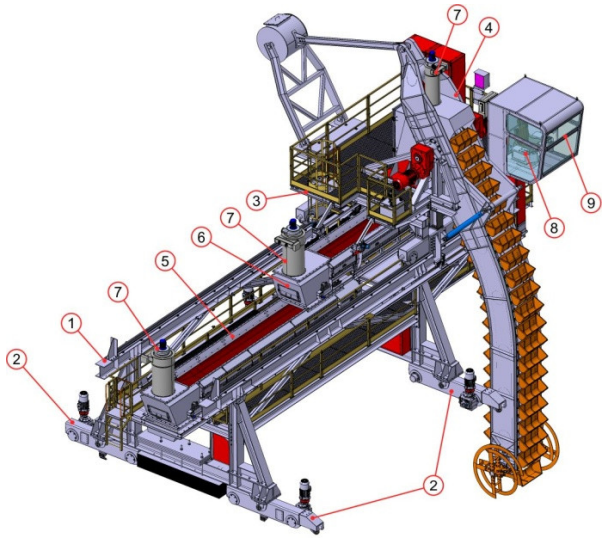

Figure 3 [6]. Basic subsystems of the S-R USKL

The gantry, Figure 4, consists of two identical frames – the rigid leg (1) and the flexible leg (2) – bearing the two main girders (3) with the tracks (4) for the positioning of the mobile trolley with the working device (WD). The gantry also supports the substructure of the tracks for the positioning of the mobile transporter (5) and the cascade discharge device (6), as well as the substructure of the walkways and ladders. The girder structure is made of standard rolled steel (grade of S235J2) profiles. The structural elements are connected with screws and welds. The static stability is ensured by the 7777 kg counterweight (7).

The movement mechanism, Figure 4, consists of two pairs of identical two-wheel bogeys (8). The joint (9) between the two-wheel bogeys and the perpendicular girders of the (9) rigid leg (1) and the flexible leg (2) equalizes the loads betwheen the wheels. One wheel of each two-wheel bogey is driven by a frequency-controlled 7.5 kW electromotor (11), which prevents the appearance of skewing. The wheels move along the tracks made of standard railway tracks S49, Figure 6.

The drivepower of the conveyor belt (5), Figure 3, is 3 kW, whereas its movement along the main girder is done by two identical 1.1 kW drivetrains.

The mobile trolley, Figure 5, bear the WD of the bucket-chain type (1), the belt conveyor (2) and the operator's cabin (3). Positioning of the trolley along the tracks on the main girders of the gantry is achieved with a positioning mechanism consisting of two end girders (4) each with two wheels, one of which is the driving wheel. They are driven by 2.2 kW frequency-regulated electromotors. The hanging conveyor (2), with the 3 kW belt drivetrain, can move along the tracks on the trolley structure. The movement is made possible by two identical 1.1 kW drivetrains. At the transfer point, there is a dedusting device (5). The working device (1), with two monoblock drivetrains with the total power of 44 kW (6), contains 43 buckets (7), each with the volume of 70 l. The nominial frequency of revolution of the drivetrain shaft of the bucket chain is 24 min^{-1}. Balancing of the working device is achieved with the 4007 kg counterweight (8), with a joint connection to the working device and the trolley structure. A shift in the position (inclination angle) of the bucket-chain boom is achieved with the pair of identical onedirectional hydrocilinders (9), which enables the loading of the material in 1-1.5 m layers, from the etages at different heights, Figure 6: etage "0" (E_0): height 1.0 m from the bottom of the storage/discharge site; etage "1" (E_1): height 1.0-2.5 m; etage "2" (E_2): height 2.5-4.0m; etage "3" (E_3): height >4.0m.

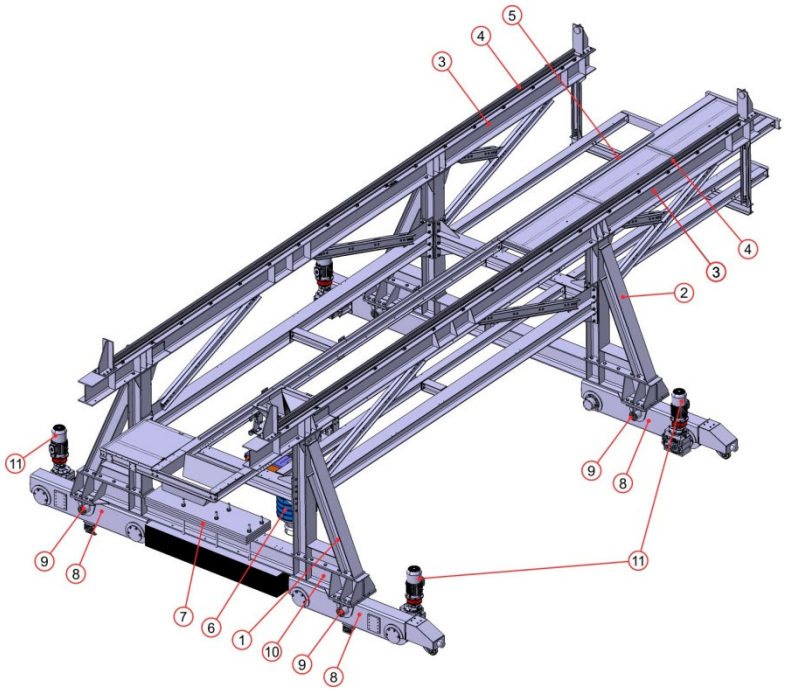

Figure 4 [6]. Gantry with the positioning mechanism

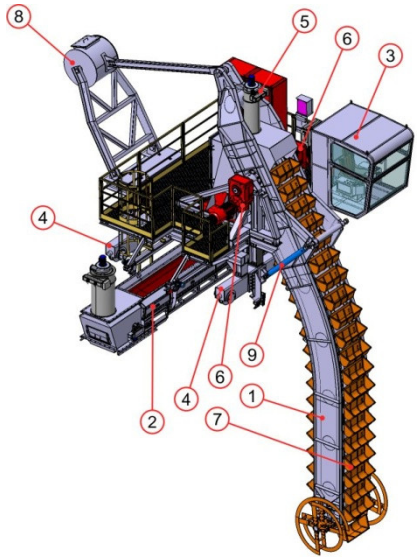

Figure 5 [6]. Trolley with the working device and the hanging conveyor

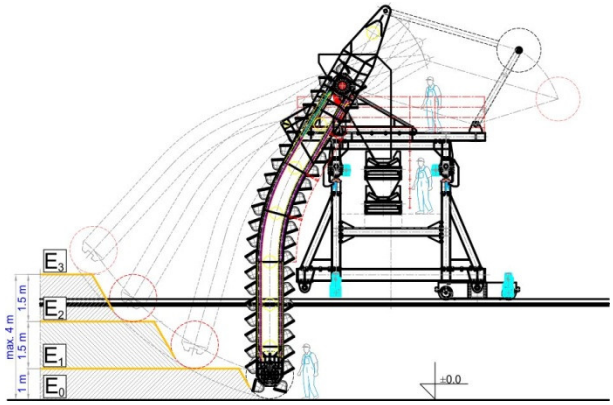

Figure 6 [6]. Heights of the etages in storage/discharge site

3. TECHNOLOGY OF OPERATION OF THE S-R USKL

The facility serves the purpose of storing crushed gypsum, created as a byproduct of desulfurization of the exaust gases at the nearby thermal power plant. The transport system within the facility consists of the analyzed stacker-reclaimer USKL and the transfer bridge TOR-1, and is able to transport the material from the storage site, mix it with ash in the process and load it onto the docked barges which then transport it away from the facility.

The crushed gypsum is brought to the discharge site (1), Figure 7, by a self-unloading truck (2). The transport of the crushed gypsum from the discharge site (1) to the storage (3) is performed by the S-R USKL (4), with the trolley and the WD (5) positioned at the end of the overhang. The discharge chute of the mobile conveyor (6) and the cascade discharge device (7) are positioned in a way that allows for even distribution of the transferred material across the crushed gypsum storage site. During the transport of the crushed gypsum from the storage site (3) to the docked barge (8), Figure 8, the trolley with the WD (5) is positioned within the span of the S-R USKL (4). The mobile belt conveyor (6), positioned at the end of the span, transfers the transported material to the intermediate conveyor (9), which then brings the material to the transfer bridge (10: "TOR-1", produced by "IVA Process Equipment" – Aranđelovac, Serbia). The crushed gypsum is, via the conveyor belt (11) located at the transfer bridge (10), transported to the discharge device (12) positioned above the barge (8).

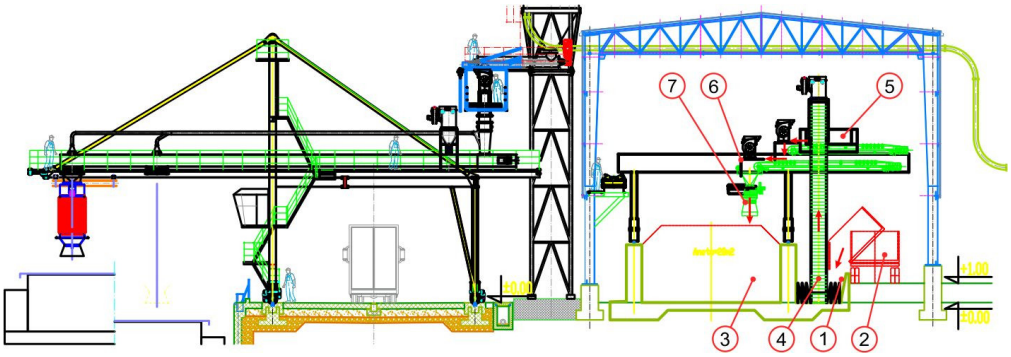

Figure 7 [6]. Transfer of the crushed gypsum from the discharge site to the storage facility

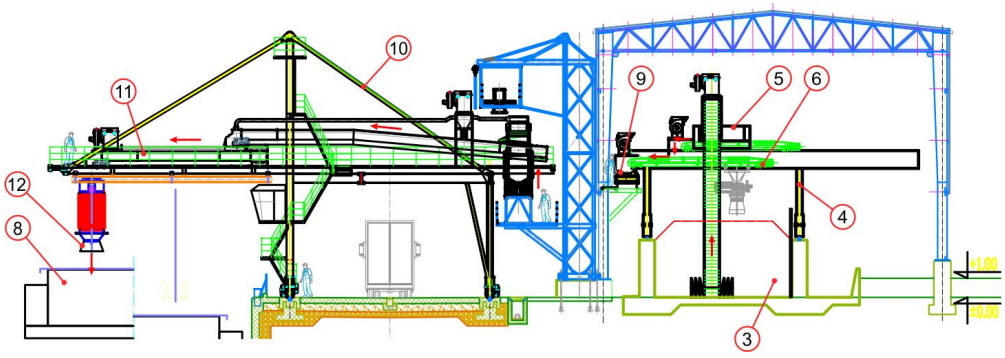

Figure 8 [6]. Transfer of the crushed gypsum from the storage facility to the docked badge

4. LFEM ANALYSES OF THE S-R USKL SUBSTRUCTURES

The FE model of the WD substructure was created by the means of discretization of the 3D model with the tetrahedron finite elements, whereas the substructures of the trolley and the gantry were modeled using beam finite elements.

The load analysis was done for:

(a) three working regimes (WRs):

- WR 1 - normal working regime (safety factor SF_1=1.5);
- WR 2 - extraordinary digging forces (safety factor SF_2=1.33);
- WR 3 - extraordinary material load+clogging of the working device chute (safety factor SF_3=1.2),

Table 2;

(b) four characteristic etage heights (EHs, Figure 6);

(c) three characteristic positions of the trolley (TPs), Figure 9.

Table 2. Working regimes

Partial loads	WR		
	1	2	3
Dead load (E)	+	+	+
Material load-buckets (F_0)	+	+	+
Material load-trolley belt conveyor (F_1)	+	+	0
Extraordinary material load-trolley belt conveyor (FF_1)	0	0	+
Material load-gantry belt conveyor (F_2)	+	+	0
Extraordinary material load-gantry belt conveyor (FF_2)	0	0	+
Encrustation-buckets (V)	+	+	+
Clogging- working device chute (VV)	0	0	+
Normal tangential digging force (U)	+	0	+
Extraordinary tangential digging force (UU)	0	+	0
Normal radial digging force (Ur)	+	0	+
Extraordinary radial digging force (UUr)	0	+	0
Dynamic effects (D)	+	+	+

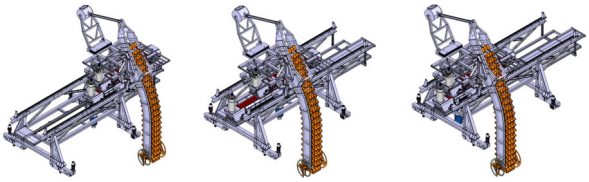

(a) (b) (c)

Figure 9 [6]. Characteristic trolley positions: (a) at the overhang (TP 1)-transport of gypsum from the discharge site to the storage; at the middle of the span (b, TP 2) and at the rigid leg (c, TP 3)-transport of gypsum from the discharge site to the barge

The LFEM analyses of the USKL substructures (working device, trolley and gantry) were done for the sets of load cases (LCs) determined by the general designation $a/b/c$, where:

- a - the identifier of the WR (the number of possible values n_a=3: a=1 for WR 1; a=2 for WR 2; a=3 for WR 3);
- b - the identifier of the EH (the number of possible values n_b=4: b=1 for E_0; b=2 for E_1; b=3 for E_2; b=4 for E_3);
- c - the identifier of the TP (the number of possible values n_c=3: c=1 for TP 1; c=2 for TP 2; c=3 for TP 3.

For the analysis of the substructure of the WD, the first two WRs are representative, i.e the number of possible values of identifier a is reduced to $n_{a,WD}$=2. Additionally, the loads on this substructure and the trolley substructure do not depend on their position relative to the gantry. Therefore, the analysis of the substructure of the WD was conducted for $n_{a,WD}n_b$=2×4=8 LCs, whereas n_an_b=3×4=12 LCs (label: a/b) were analyzed for the trolley substructure. Identification of the stress-displacement fields of the gantry substructure was performed for the total of $n_an_bn_c$=3×4×3=36 LCs (label: $a/b/c$).

Values of the permissible stresses, Table 3, were determined according to the expression $\sigma_{per,i}=\sigma_{YS}/SF_i$, i=1,2,3, where σ_{YS}=235 MPa is the minimal yield stress value for the steel grade of S235J2.

Values of the permissible displacements of the gantry substructure depend on the TP:

- for TP 1: $f_{per,TP1}=l_o/200=5880/200=29.4$ mm, where l_o=5880 is the length of the overhang;
- for TP 2: $f_{per,TP2}=l_s/600=8000/600=13.3$ mm, where l_o=5880 is the length of the span.

The permissible vertical wheel loads on the trolley and the gantry are [6]:

- for WR 1: $V_{W,per}$=212.0 kN;
- for WR 2: $V_{W,per}$=239.1 kN;
- for WR 3: $V_{W,per}$=265.0 kN.

The stress fields of the analyzed substructures and the respective displacements of the gantry susbstructure, in the representative LCs, are shown in Figures 10-12, whereas the results of the calculations, for all considered LCs, are given in Tables 4-6.

Table 3. Permissible stresses

WR	σ_{per} (MPa)
1	156.7
2	176.7
3	195.8

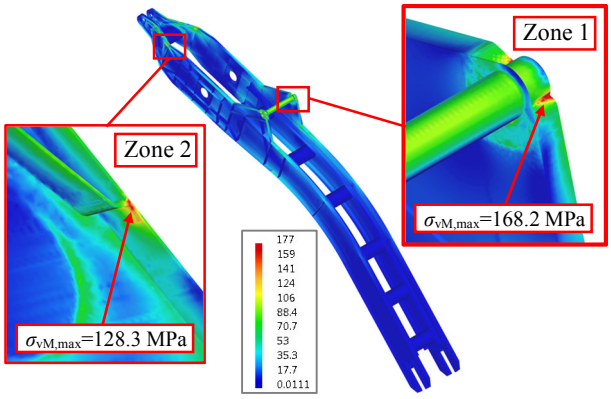

Figure 10 [6]. Von Mises stress field of the working device substructure: LC 2/4

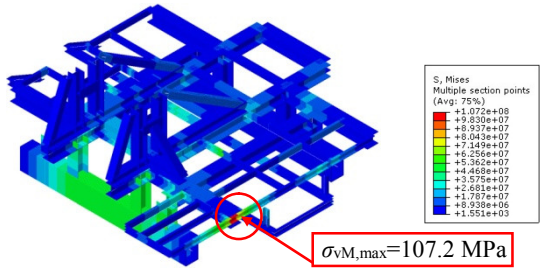

Figure 11 [6]. Von Mises stress field of the trolley substructure: LC 2/4

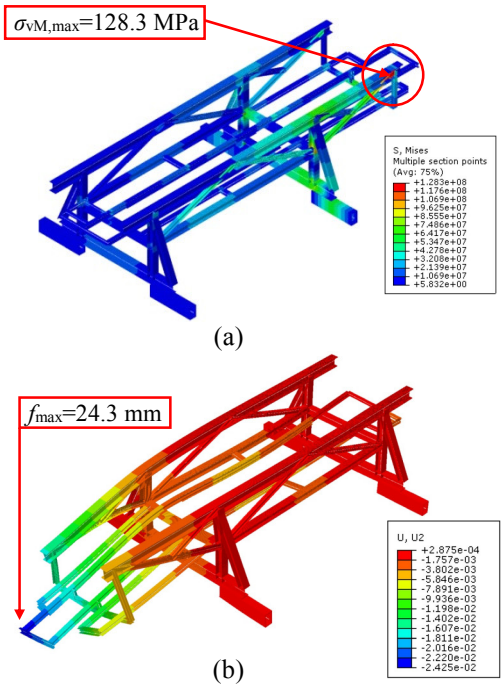

Figure 12 [6]. Gantry substructure in LC 2/4/1: (a) von Mises stress field; (b) vertical displacement field

Table 4. Working device substructure: the maximum von Mises stresses ($\sigma_{vM,max}$) vs permissible stresses (σ_{per})

LC	$\sigma_{vM,max}$ (MPa)		σ_{per} (MPa)
	zone 1	zone 2	
1/1	62.3	106.6	156.7
1/2	103.2	128.2	
1/3	135.7	142.1	
1/4	155.8	150.6	
2/1	70.3	102.1	176.7
2/2	113.4	121.6	
2/3	147.4	133.8	
2/4	168.2	141.3	

Table 5. Trolley substructure: the maximum von Mises stresses ($\sigma_{vM,max}$) vs permissible stresses (σ_{per})

LC	$\sigma_{vM,max}$ (MPa)	σ_{per} (MPa)
1/1	105.0	156.7
1/2	106.0	
1/3	106.7	
1/4	106.9	
2/1	105.2	176.7
2/2	106.2	
2/3	107.0	
2/4	107.2	
3/1	105.2	195.8
3/2	106.1	
3/3	106.8	
3/4	107.1	

The intensities of the vertical wheel loads on the trolley and the gantry, Figures 13, representative for the proof of their bearing capacity, and the proof of static stability, are given in Tables 7 and 8.

Table 6. Trolley substructure: maximum von Mises stresses ($\sigma_{vM,max}$) vs permissible stresses (σ_{per}) and maximal displacements (f_{max}) vs permissible displacements (f_{per})

LC	$\sigma_{vM,max}$	σ_{per}	f_{max}	f_{per}
	MPa		mm	
1/1/1	100.2	156.7	21.6	29.4
1/1/2	71.6		10.6	13.3
1/1/3	74.1		10.3	
1/2/1	111.4		22.5	29.4
1/2/2	80.1		10.6	13.3
1/2/3	77.9		10.3	
1/3/1	119.9		23.3	29.4
1/3/2	86.6		10.6	13.3
1/3/3	80.9		10.3	
1/4/1	125.0		23.7	29.4
1/4/2	90.6		10.6	13.3
1/4/3	82.7		10.3	
2/1/1	102.4	176.7	22.0	29.4
2/1/2	73.6		10.6	13.3
2/1/3	75.6		10.4	
2/2/1	114.1		23.0	29.4
2/2/2	82.5		10.6	13.3
2/2/3	79.6		10.3	
2/3/1	123.1		23.8	29.4
2/3/2	89.4		10.6	13.3
2/3/3	82.8		10.3	
2/4/1	128.3		24.3	29.4
2/4/2	93.4		10.7	13.3
2/4/3	84.6		10.3	
3/1/1	104.9	195.8	22.7	29.4
3/1/2	74.9		11.3	13.3
3/1/3	77.0		11.0	
3/2/1	116.0		23.6	29.4
3/2/2	83.4		11.3	13.3
3/2/3	80.8		11.0	
3/3/1	124.6		24.4	29.4
3/3/2	89.9		11.3	13.3
3/3/3	83.8		11.0	
3/4/1	129.6		24.8	29.4
3/4/2	93.9		11.3	13.3
3/4/3	85.6		11.0	

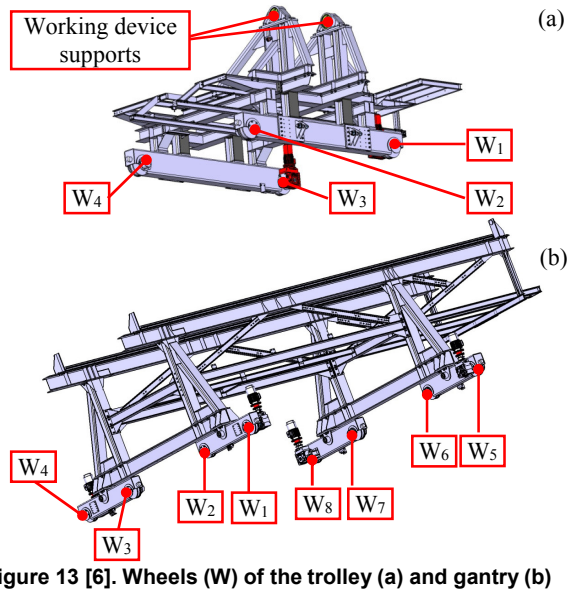

Figure 13 [6]. Wheels (W) of the trolley (a) and gantry (b)

Table 7. Trolley wheel loads

LC	V_{Wi}, i=1,2,3,4 (kN)				$V_{W,per}$ (kN)
	W_1	W_2	W_3	W_4	
1/4	168.6	149.2	29.8	23.8	212.0
2/4	173.8	154.4	26.1	20.1	239.1
3/4	175.2	154.6	33.5	26.8	265.0

Table 8. Minimal gantry wheel loads

LC	V_{Wi}, i=1,2,3,4 (kN)			
	W_1	W_2	W_3	W_4
1/4/1	17.2	16.2	33.0	33.0
2/4/1	16.6	15.6	33.3	33.3
3/4/1	15.7	14.7	31.8	31.8

Table 9. Maximal gantry wheel loads

LC	V_{Wi}, i=5,6,7,8 (kN)				$V_{W,per}$ (kN)
	W_5	W_6	W_7	W_8	
1/1/1	194.5	193.5	141.6	141.6	212.0
1/4/1	219.0	218.1	116.9	116.9	212.0
2/4/1	222.8	221.8	115.0	115.0	239.1
3/4/1	227.3	226.3	122.9	122.9	265.0

5. DISCUSSION AND CONCLUSION

The complexity of the analyses of the substructures of the stacker-reclaimer is the consequence of, among other factors, its variable geometric configuration: (a) a change in the position of the working device relative to the trolley; (b) a change in the position of the trolley relative to the gantry. Based on the presented results of the finite element analyses, the following has been concluded:

- in all the working regimes, the highest stresses in the working device substructure, as well as the trolley substructure, occur during the loading of the gypsum from the fourth etage;
- in all the considered load cases, the substructures of the working device and the trolley satisfy the strength criterion: the maximum values of the stresses are lower than the corresponding permissible values, Tables 4 and 5;
- in all the working regimes and etage heights, the highest stresses and displacements of the gantry substructure occur when the tolley is at the overhang;
- in all the considered load cases, the gantry substructure satisfies the criterions of strength and displacements: the maximum values of stress and displacement are lower than the corresponding permissible values, Table 6;
- the maximal and the minimal loads on the trolley wheels occur during the loading of the gypsum from the fourth etage, Table 7;
- the maximum loads of the trolley wheels are lower than permissible, Table 7;
- the maximal and minimal loads of the wheels on the gantry occur during the loading of the crushed gypsum from the fourth etage when the trolley is at the overhang, Tables 8 and 9;
- the average maximal load of the wheel on the gantry, in the normal working regime,

$$V_{W5,mean} = \frac{2V_{W5,LC\ 1/4/1} + V_{W5,LC\ 1/1/1}}{3} = \\ = \frac{2\times 219.0 + 194.5}{3} = 210.8 \text{ kN},$$

is lower than permissible, $V_{W,per,WR\ 1}$=212.0 kN, Table 9; in other working regimes, the maximal loads of the wheels on the gantry are lower than permissible, Table 9;

- even in the most unfavorable cases, the wheels on the trolley and the gantry are under loads, Tables 7 (wheels W3 and W4) and Table 8, meaning that the required conditions of static stability of the trolley with the working device, as well as the stacker-reclaimer in its entirety, have been met (the proof of safety against overturning was conducted in accordance with the code F.E.M. SECTION II [6]).

Finally, a two-year failureless exploitation of the analyzed stacker-reclaimer acts as an indirect validation of not only the presented results, but the entire design project and the technology of manufacture and montage.

ACKNOWLEDGMENT

This work is a contribution to the Ministry of Education, Science and Technological Development of Serbia funded project "Integrated research in the fields of macro, micro and nano mechanical engineering" (Contract number: 451-03-68/2022-14/200105).

REFERENCES

[1] *Stacking, blending, reclaiming of bulk materials*, edited by R.H. Wohlbier, Trans Tech Publications, Clausthal, 1977.

[2] Gašić, V., Zrnić, N., Bošnjak, S.: Concept and main analysis problems of modern stackers-reclaimers, Proceedings of the 8th International Conference on Accomplishments in Electrical, Mechanical and Informatic Engineering DEMI 2007, University of Banja Luka-Faculty of Mechanical Engineering, Banja Luka, Bosnia and Herzegovina, pp. 29-34, 2007.

[3] Bošnjak, S. and Zrnić, N.: Dynamics, failures, redesigning and environmentally friendly technologies in surface mining systems, Arch. Civ. Mech., Vol. 12, No. 3, pp. 348-359, 2012.

[4] Bošnjak, S., Gašić, V., Petković, Z.: Determination of resistances to coal reclaiming at bridge - type stacker – reclaimer with bucket chain booms, FME Trans., Vol. 33, No. 2, pp. 79 – 88, 2005.

[5] Bošnjak, S., Gnjatović, N., Milenović, I., Stefanović, A., Urošević, M.: Strength calculation of the stacker-reclaimer "USKL" structure (in Serbian), realized for "IVA Process Equipment" - Arandjelovac (Serbia), University of Belgrade-Faculty of Mechanical Engineering, Belgrade, 2019.

[6] FEM SECTION II: Rules for the design of mobile equipment for continuous handling of bulk materials. De La Federation Europeenne de la Manutention, Brussels, Belgium, 1997.